INL/CON-22-67838-Revision-1

Corrosion evaluation of metal foams in eutectic molten salts for high temperature latent heat energy storage application

November 2022

Hansol Kim, Joseph Seo, Yassin A Hassan, Sunming Qin, Minseop Song, Jeremy Lee Hartvigsen, Jun Soo Yoo

Changing the World's Energy Future

Idaho National Laboratory

INL is a U.S. Department of Energy National Laboratory operated by Battelle Energy Alliance, LLC

INL/CON-22-67838-Revision-1

Corrosion evaluation of metal foams in eutectic molten salts for high temperature latent heat energy storage application

Hansol Kim, Joseph Seo, Yassin A Hassan, Sunming Qin, Minseop Song, Jeremy Lee Hartvigsen, Jun Soo Yoo

November 2022

Idaho National Laboratory
Idaho Falls, Idaho 83415

http://www.inl.gov

Prepared for the
U.S. Department of Energy
Under DOE Idaho Operations Office
Contract DE-AC07-05ID14517

Corrosion Evaluation of Metal Foams in Eutectic Salts for Selection of High-Temperature Heat Storage Medium

Hansol Kim*, Joseph Seo*, Yassin A Hassan*
JunSoo Yoo†, Minseop Song†, Sunming Qin†, Jeremy Hartvigsen†

** Texas A&M University, Department of Nuclear Engineering, 3133 TAMU, College Station, TX 77843*
†Idaho National Laboratory, 2525 North Fremont Ave, Idaho Falls, ID 83415

INTRODUCTION

With the recent development of the 4th generation nuclear power plant, research on coupling the heat generated from nuclear reactor to industrical process is receiving great attention. Idaho National Laboratory (INL) has prposed various research needs in the "Integrated Energy Systems: 2020 Roadmap" with the goal of industrial use of the high temperature heat of 550 degrees or higher generated by the advanced nuclear reactors [1]. A high-temperature heat pipe-integrated Thermal Energy Storage (TES) research, recently proposed by INL, to connect the emerging micro nuclear reactors to the microgrid is in the same vein [8]. Texas A&M University (TAMU) and INL are collaborating to develop and demonstrate a novel latent heat-based TES design called HITB (Heat pipe-Integrated Thermal Battery). HITB is a high-temperature TES system that stores and transports heat as needed between advanced reactors (heat source) and industrial processes (heat customers). The HITB utilizes high-temperature heat pipes with a moving mechanism for charging and discharging the heat. Figure 1 shows the design concept of the HITB system.

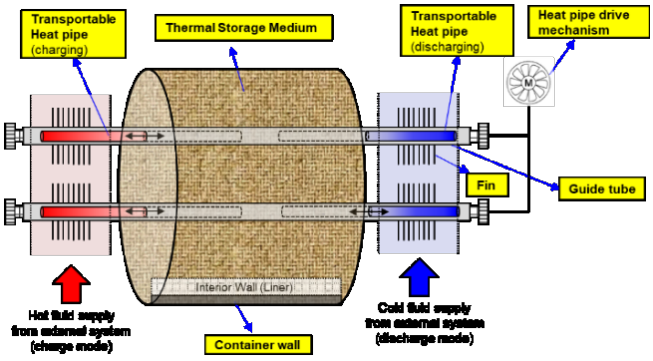

Fig. 1. Heat-pipe Integrated Thermal Battery (HITB): Key Design Concept and Components[8].

As part of the small-scale experimental demonstration research for HITB, experiments were performed to evaluate the corrosion behavior between the candidate TES media i.e., eutectic salts, and the internal metal structures. In HITB, the use of metal foam structure is considered inside a TES tank to overcome eutectic salts' poor heat transfer characteristics. The TES tank wall is made of SS-316. Considering the current target operating temperature of the HITB, 450500℃, several eutectic salts having a melting temperature near 450 ℃ were selected for the experiment. Especially molten chloride salts and molten fluoride salts are considered promising candidates due to their high melting temperature, thermal stability, and high latent heat of fusion. For the internal metal structure inside a TES tank, copper and aluminum foam structures, which have high thermal conductivity and large heat transfer area, were selected and investigated as the candidate materials to enhance the charging/discharging efficiency of the TES medium [2]. In the literature, the corrosion studies have been conducted with various eutectic salts on materials with very high corrosion resistance regardless of their thermal conductivity such as SS304, SS316, Hastelloy, Inconel 625, and Incoloy 800H [3-6]. In addition, porous materials with high thermal conductivity, made of such as copper and aluminum, have only been tested in the fluids such as paraffin or water at relatively low temperatures, but high-temperature corrosion tests with various eutectic salts were not performed yet.

In this study, we selected three different types of fluoride and chloride eutectic salts, all of which have melting temperatures around 450 ℃, and investigated the corrosion behavior of the metal structures made of copper and aluminum within the candidate eutectic salts. Specifically, the high-temperature corrosion characteristics of metal alloys, such as C10100 foam, C10100 plate, 6101 alloy foam, and SS316 plate, were investigated while immersed in the candidate eutectic salts such as $MgCl_2$-NaCl, $CaCl_2$-NaCl, and FLiNaK. The chemical compositions of the specimens of SS316, C10100, and 6101 alloys are listed in Table 1. To quantify and compare the corrosion behaviors of each metal, the corrosion rate [mm/yr] and average mass loss [mg/mm^2] were calculated as follows [7]:

$$CR = \frac{K \cdot W}{A \cdot \rho \cdot t} \quad (1)$$

$$\text{Mass loss} = \frac{W}{A} \quad (2)$$

where K [-] is a constant (87,600), W [g] is the sample mass loss, A [cm^2] is the initial surface area of the sample, ρ [g/cm^3] is the density of the sample, and t [hours] is the exposure time.

A total of 20 tests for SS316 coupons and ten tests for C10100 coupons were performed to ensure the repeatability of the present measurements. Since it is difficult to completely remove the salt inside metal foam due to the complex inner structure of the metal foam, only the surface condition was observed with a microscopy and scanning electron microscopy (SEM) image, except for measuring the

corrosion rate and average mass loss.

EXPERIMENTAL SETUP

The experiments were conducted in three candidate molten salts, $MgCl_2$-NaCl (43.1-56.9 mol%), FLiNaK (46.5-11.5-42 mol%) and $CaCl_2$-NaCl (52.1-47.9 mol %). The $MgCl_2$ (Sigma-Aldrich, 7786-30-3, > 98.0 %) and NaCl (Sigma-Aldrich, 7647-14-5, >99%) salts for $MgCl_2$-NaCl mixture, and LiF Alfa Aesar, 7789-24-4, >98.5%), KF (Alfa Aesar, 7789-23-3, >99%), NaF (Alfa Aesar, 7681-49-4, >99%) for FLiNaK, $CaCl_2$ (Sigma-Aldrich, 10043-52-4, > 97%) and NaCl (Sigma-Aldrich, 7647-14-5, >99%) salts for $CaCl_2$-NaCl mixture were used in this study. Salt preparation was done in the glovebox. The glovebox condition maintained an extremely low concentration level of under one ppm of oxygen and moisture. The mixing process took place in a glove box. Ar gas connection for flushing was applied, and a high-temperature immersion test was performed. C10100 foam, C10100 plate, Aluminum Alloy 6101 foam, and SS316 plate were selected as the samples for the metal form and casing candidates. Pores per inch property for metal foams were selected at 20 PPI. Each sample was washed with DI water in the ultra-sonicator and rinsed in acetone. The samples were dried, the surface area measured, and weighted using the scale of $\pm 0.001g$ of accuracy. The corrosion test for each coupon in each molten salt was performed at 550℃ for a duration of 120 hours in the furnace (2100W digital control melting furnace, VEVOR). After the immersion test, each sample was sonicated with DI water for 3 hours to remove the remaining salts and rinsed with acetone (600W, 40kHz). The samples were dried, weighted and calculated the corrosion rate using the scale, which is $\pm 0.001g$ of accuracy. Surface experiments were observed before and after, and microscopic morphologies were also performed using scanning electron microscope(SEM).

TABLE I. Chemical compositions of the specimens (in mass %)

C10100	**Cu**	**Ag**	**Pb**	**O**	**As**	**Sb**
	99.9	0.0025	0.0005	0.0005	0.0005	0.0004
6101Alloy	**Al**		**Mg**		**Si**	
	98.9		0.60		0.50	
SS316	**Fe**	**Cr**	**Ni**	**Mn**	**Mo**	**Cu**
	58.23-73.61	16-18.5	10-15	0-2	0-3	0-1
	N2	**Si**	**S**	**Ti**	**P**	
	0-0.1	0-1	0.35	0.7	0-0.045	

TABLE II. Thermal properties of the specimens

Samples	**C10100**	**6101Alloy**	**SS316**
Melting point [°C]	1082	588	1375-1400
Thermal conductivity [W/m°K]	226	218	16.3
Thermal expansion [µm/µm/°C]	9.8	23	15.9

Results and Discussion

After 120 hours of 550 C corrosion test, we compared surface on two chloride salts and fluoride salts ($MgCl_2$-NaCl, $CaCl_2$-NaCl, FLiNaK) for the metal foam structures (6101 Alloy, C10100). Fig. 2 shows the results of the surfaces of C10100 foam and 6101 alloy foam before and after. 6101 Alloy was most severely corroded in the case of the foam tested in $MgCl_2$-NaCl, followed by FLiNaK corrosion, and the least surface roughness was not changed in the case of $CaCl_2$-NaCl. For $MgCl_2$-NaCl, it is known that the HCl gas generated due to the impurity generated by the very strong hygroscopic properties of $MgCl_2$ reacted violently with the aluminum. In the case of C10100 foam, it maintained a relatively better condition than 6101 Alloy in all eutectic salts. However, the oxide film on the surface disappeared, the surface roughness increased, and the string of the foam structure was broken in the case of $MgCl_2$-NaCl. These findings confirmed that it was difficult to use aluminum (6101 Alloy) in the form of metal foam to improve the heat transfer characteristics of the thermal storage medium designed for HITB. In the case of copper (C10100), the metal structure used in $CaCl_2$-NaCl was visually confirmed to be the most corrosion resistant.

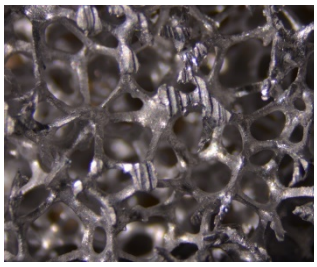

(a) 6101 Alloy foam (before immersion test)

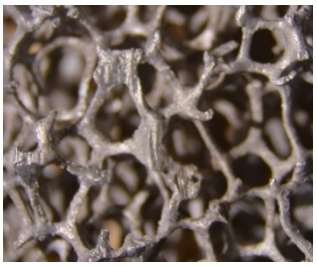

(b) 6101 Alloy foam in $CaCl_2$-NaCl

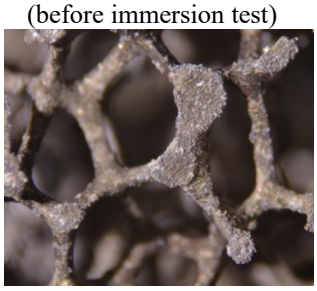

(c) 6101 Alloy foam in FLiNaK

(d) 6101 Alloy foam in $MgCl_2$-NaCl

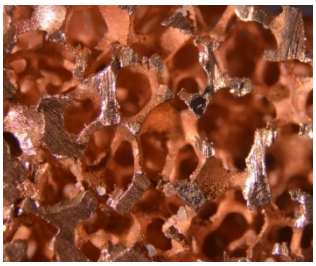
(e) C10100 Alloy foam (before immersion test)


(f) C10100 Alloy Foam in $CaCl_2$-NaCl

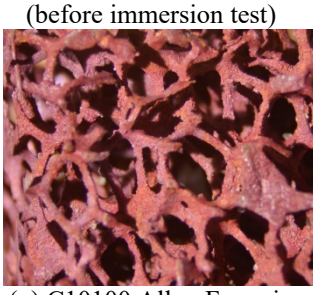
(g) C10100 Alloy Foam in FLiNaK

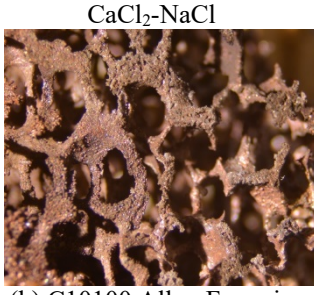
(h) C10100 Alloy Foam in $MgCl_2$-NaCl

Fig. 2. Initial and corrosion-tested metal form coupons

Corrosion rate and average mass loss

Table I shows the initial surface areas, masses, final masses, average mass losses, and corrosion rate of metal plates (C10100, SS316) in the $CaCl_2$-NaCl mixture. The average corrosion rates of C10100 and SS316 in $CaCl_2$-NaCl salts at 550 C for 120 hours are 0.768 and 0.680, respectively.

TABLE III. Coupon data

	C10100	**SS316**
Surface area [cm^2]	0.839	0.923
Initial mass [g]	0.279	0.281
Final mass [g]	0.272	0.275
Average mass loss [mg/cm^2]	9.366	7.443
Corrosion rate [mm/yr]	0.768	0.680

Microscopic observations

Figure 3 (a) and (b) represent the morphologies of the SS 316 surfaces before and after the immersion test using $CaCl_2$-NaCl salts. Fig. 3(b) shows the rough surface with various holes. As shown in Fig. 4, In the C10100 foam structure immersed in $CaCl_2$-NaCl, holes of less than one μm were found. In $MgCl_2$-NaCl, holes, and cracks over 2um were found, and in FLiNaK, holes over 2um were found. In the 6101 alloy foam structure in Fig. 5, much larger holes were formed on the surface than in the case of the previous C10100. The roughness of the surface information makes it difficult to illustrate how the metal of the corrosion test has changed. The results, however, plainly reveal that corrosion has occurred on the surface.

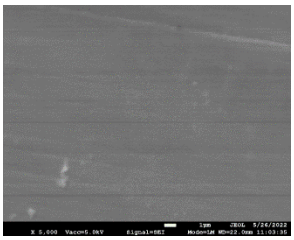
(a) before

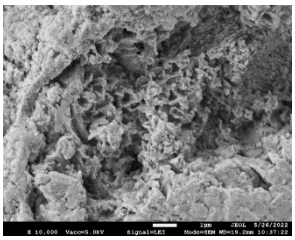
(b) after

Fig. 3. SEM images of SS 316 plate before and after immersion in salts, $CaCl_2$-NaCl

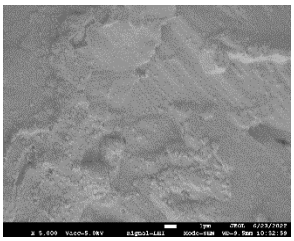
(a) before

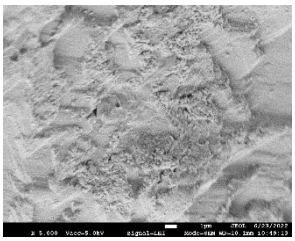
(b)

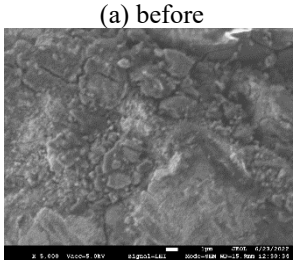
(c)

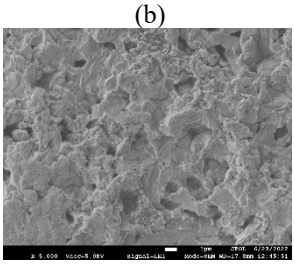
(d)

Fig. 4. SEM images of C10100 foam structure (a) before and after immersion in salts, (b) $CaCl_2$-NaCl, (c) $MgCl_2$-NaCl, (d) FLiNaK

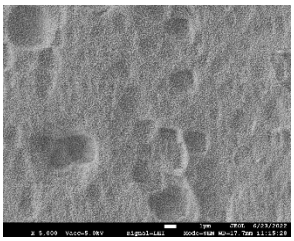
(a) before

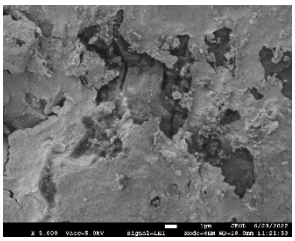
(b) after

Fig. 5. SEM images of 6101 Alloy foam structure (a) before and (b) after immersion in salts, $CaCl_2$-NaCl

Selection of thermal energy storage medium

Table IV examines each eutectic salt mixture's thermal characteristics, cost, and corrosion of porous structures. The operating temperature range for HITB is 450-500 degrees Celsius. The larger the latent heat of fusion and specific heat capacity, the larger the thermal energy storage. Furthermore, the higher the thermal conductivity, the smaller the temperature gradient that can be efficiently charged and discharged, increasing total system efficiency. The price of salts is also an essential factor to be considered for economic feasibility. Furthermore, eutectic salts should be

chosen with the corrosivity-resistance of the porous structure in order to increase the designed thermal conductivity in the HITB system in consideration. FLiNaK and FLiBe, famous for fluoride salts, are good candidates, but due to the sharp rise in the price of LiF recently, they are excluded for economic reasons to be applied to large-capacity thermal energy storage. On the other hand, chloride salts are very cheap and easy to obtain, have a high melting temperature, and have a high latent heat of fusion, so they are recently in the spotlight as a phase change material. However, because of the hygroscopic nature of chloride salts, HCl gas due to impurity is easy to be released and is particularly vulnerable to corrosion. As a result of comparing $MgCl_2$-NaCl and CaCl2-NaCl, $CaCl_2$-NaCl salts might be chosen as the most reasonable mixture for HITB in this study.

TABLE IV. Eutectic salts mixtures and properties [2, 8]

	FLiNaK	**$MgCl_2$-NaCl**	**$CaCl_2$-NaCl**
x_A-x_B-(x_C) (mol %)	46.5-11.5-42	43.1-56.9	52.1-47.9
Tm (°C)	454	450	504
ΔH_{fusion} (kJ/kg)	187.7	431	265
Thermal conductivity (W/m K)	0.80	-	1.02
Specific heat capacity (kJ/kg K)	1.88	0.91	0.84
Cost ($/kg)	450	6.55	9.89
Corrosion for C10100	medium	high	low

SUMMARY

In this study, immersion tests were conducted on three candidate molten salts, MgCl2-NaCl (43.1-56.9 mol%), FLiNaK (46.5-11.5 mol%), and CaCl2-NaCl (52.1-47.9 mol%) mixtures, with different metal foam candidates. 550 °C corrosion tests of C10100, 6101 Alloy, and SS316 were performed for 120 hours and compared by investigating the corrosion rate, average mass loss, and microscopic observation. The average corrosion rates of C10100 and SS316 in CaCl2-NaCl salts at 550 °C for 120 hours are 0.768 and 0.680, respectively. As a result of observation for SS316 with SEM, rough surfaces with various sized holes were found. As a result of examining thermal properties, cost, and corrosion behavior, the C10100 metal foam structure in CaCl2-NaCl was observed as the most suitable salts-metal foam material combination in this study.

ACKNOWLEDGEMENTS

This research is funded by the Idaho National Laboratory (INL) 's Directed Research and Development (LDRD) program. The support is gratefully acknowledged. Use of the Texas A&M University Materials Characterization Core Facility (RRID: SCR_022202) is acknowledged.

REFERENCES

1. S. M. Bragg-Sitton, C. Rabiti, R. D. Boardman, J. O'Brien, T. J. Morton, S. Yoon, J. Yoo, K. Frick, and P. Sabharwall. "Integrated Energy Systems: 2020 Roadmap." INL EXT-20-57708, Idaho National Laboratory (2020).
2. G. Wei et al., "Selection principles and thermophysical properties of high temperature phase change materials for thermal energy storage: A review", Renewable and Sustainable Energy Rev., 81 (2018), pp.1771-1786
3. Y.S. Li, M. Spiegel, "Models describing the degradation of Fe-Al and Ni-Al alloys induced by $ZnCl_2$-KC1 melt at 400-450 °C", Corros. Sci., 46 (2004), pp. 2009-2023
4. Y. Lu, Cheng B, J. Wang, "Corrosion behavior of Cr, Fe and Ni based superalloy in molten NaCl", Rare Met. Mater. Eng., 43 (2014), pp. 17-23
5. K. Vignarooban, P. Pugazhendhi, R.C. Tucker, "Corrosion resistance of Hastelloys in molten metal-chloride heat-transfer fluids for concentrating solar power applications", Sol. Energy, 103 (2014), pp. 62-69
6. Liu B, X. Wei, W. Wang, "Corrosion behavior of Ni-based alloys in molten NaCl-$CaCl_2$-$MgCl_2$ eutectic salt for concentrating solar power", Sol. Energy Mater. Sol. Cell., 170 (2017), pp. 77-86
7. J.R. Scully and R.G. Kelly, "Methods for Determining Aqueous Corrosion Reaction Rates, Corrosion: Fundamentals, Testing, and Protection," Vol 13A, ASM Handbook, ASM International, 2003, p 68–86
8. Serrano-Lopez et al., "Molten salts database for energy applications", Chemical Engineering and Processing: Process Intensification, 73 (2013), pp. 87-102
8. Yoo et al., “High-Temperature Latent Heat Storage System using Transportable Heat Pipes for Versatile Integration with Emerging Microreactors”, 2022 ANS Winter Meeting and Technology Expo